IL NUOVO CIMENTO Vol. 29 C, N. 2 Marzo-Aprile 2006
DOI 10.1393/ncc/i2005-10061-1

Limited area energy budget during a life cycle of Genoa cyclone (18-21 November 1999)

I. H. Bulić(*)

Andrija Mohorovičić Geophysical Institute, Faculty of Science, University of Zagreb Horvatovac bb, 10000 Zagreb, Croatia

(ricevuto il 17 Giugno 2005; revisionato l'1 Dicembre 2005; approvato il 5 Dicembre 2005; pubblicato online il 17 Febbraio 2006)

Summary. — A case of deep and rapid cyclogenesis over the Gulf of Genoa and its impact on a limited area energy budget are examined in this paper. Energy components, including boundary and generation terms, are calculated for the period 18-21 November 1999 over a limited region in which this disturbance is the major synoptic-scale feature. The energy contents and their changes through the studied atmospheric volume are discussed in the course of the cyclone's development. The combined boundary pressure work and dissipation terms of the zonal and eddy kinetic energies, as well as generation terms of zonal and eddy available energies, are computed as residuals. Data of ALADIN/LACE model are used as input fields for calculations. Formation of the cyclone under study initiated in the upper atmospheric levels. At the initial stage of its development, energy conversion $C(K_{\mathrm{Z}}, K_{\mathrm{E}})$ was intense. Thus, zonal flow acted as a source of eddy kinetic energy. The disturbance was induced by a very strong wind shear and the progress of the vortex toward the lower atmospheric layers was associated with downward eddy kinetic energy transport (from the jet stream level toward the surface). Simultaneously, the upward transport of both zonal and eddy available energies (from the lower and middle troposphere toward the upper levels) was present. The disturbance was a consequence of very strong wind shear and it was evident how it progressed toward the lower atmospheric layers. As the vortex reached the ground, energy conditions allowed its possible further growth there. In spite of that, the surface cyclone lifetime was very short due to dynamical conditions that attenuated cyclone development.

PACS 92.60.-e – Meteorology.

1. – Introduction

Since Lorenz [1] introduced the concept of energy cycle to the theory of general circulation, the energetic of atmospheric dynamics has been studied extensively. As he suggested, wind field can be resolved into mean zonal motion and eddies superimposed on it. Therefore, kinetic energy (K) is partitioned into two types: zonal kinetic energy (K_{Z}) and eddy kinetic energy (K_{E}). Available potential energy (A) depends on temperature

(*) E-mail: iherceg@irb.hr

variances. Similarly as the motion, the variance of temperature field can be resolved into variances of zonally averaged temperature and variances of temperature within latitude circles. Thus, the available potential energy can also be partitioned into zonal available potential energy (A_Z) and eddy available potential energy (A_E). These energy forms are physically connected and one type of energy may be a source or a sink of the other type. The energy cycle of general circulation consists of generation, transformation, conversion and dissipation of the mean and eddy energies. Although Lorenz's global energy cycle refers to the whole atmosphere, some investigators have used his concept to study the energetics of particular atmospheric layers, such as the stratosphere [2-4]. Also, an appreciable effort has been made to obtain the energy characteristics of the monsoon circulation and to evaluate the energy budget of associated cyclones [5-8]. As was emphasized by Lorenz [1], large-scale eddies have an important role in the maintenance of the general circulation against dissipative effects. Smith [9] pointed out synoptic scale systems as significant components of the energy cycle in the middle latitudes. As indicated by his study, cyclone systems can act as centres of strong energy processes and thus, influence the general circulation of the middle latitudes.

The region south of the Alps is a very interesting cyclogenetic area with a pronounced sea thermal effect. This is an important factor in the energy cycle and it participates in the generation mechanisms of eddy available potential energy (A_E). Further, the Alps present an obstacle to the north-western flow, which favours lee cyclogenetic processes. Alpert *et al.* [10] suggest that thermal effect is significant only during the summer months, while lee cyclogenesis has the major role during winter.

By an earlier limited-area energetic study, Herceg [11] has shown that even a simple calculation over a small region during a cyclone development over the Gulf of Genoa can give logical and explainable results. But that study did not examine the whole energy cycle and did not include boundary transports.

The aim of the present study is to provide the temporal and spatial evolution of energy components during the cyclone development. Furthermore, one of the goals is to investigate whether an intense Genoa cyclone development has recognizable influence on energetics over the domain covered by ALADIN/LACE(1) model. It is a numerical model which is routinely used for operative purposes in Meteorological and Hydrological Service of Croatia so it is also used in this study.

It turned out that influence of the cyclone development may be recognized in the energy budget calculated over extremely small domain. An attempt has been made to investigate the vertical transfer of energy throughout the atmosphere. Furthermore, an estimation of the possible mechanism of the cyclone formation is one of the goals of this study. The results also show that the geographical position of the cyclone relatively to the domain of the model has an impact on the calculation of energy components.

It is important to note that no attempt is made to define the energy budget of this particular cyclone. Rather, the estimated energy processes in the limited region are examined in terms of their contribution and relationship to global energy processes. The theoretical justification for such approach is discussed by Smith [12] and Johnson [13].

(1) Aire Limitée Adaptation Dinamique et Dévelopment InterNational/Limited Area model for Central Europe.

2. – Energy equations

In the present paper the energetics during the cyclone formation over the Gulf of Genoa are studied. The energy equations that are used to calculate amounts of the energy forms and their conversions and transformations, are based on the equations given by Lorenz [1] but they also include the mass exchange through the boundaries.

For an arbitrary variable F, the notation $[F]$ and $\overline{F}$ is applied for zonal and area average, respectively. The departure from the zonal average $(F-[F])$ and the departure of the zonal average from the area average $([F]-\overline{F})$ are denoted as F^* and $[F]''$, respectively. By the use of the mentioned notation, various energy components are given by the following equations:

$$A_{\mathrm{Z}} = \int\limits_{p_{\mathrm{TOP}}}^{p_0} \frac{\overline{[T]''^2}}{2\sigma} \mathrm{d}p\,, \tag{1}$$

$$A_{\mathrm{E}} = \int\limits_{p_{\mathrm{TOP}}}^{p_0} \frac{\overline{T^{*2}}}{2\sigma} \mathrm{d}p\,, \tag{2}$$

$$K_{\mathrm{Z}} = \int\limits_{p_{\mathrm{TOP}}}^{p_0} \frac{\overline{[u]^2+[v]^2}}{2g} \mathrm{d}p\,, \tag{3}$$

$$K_{\mathrm{E}} = \int\limits_{p_{\mathrm{TOP}}}^{p_0} \frac{\overline{u^{*2}+v^{*2}}}{2g} \mathrm{d}p\,, \tag{4}$$

where K_{Z} and K_{E} are the zonal and eddy kinetic energy, respectively, and A_{Z} and A_{E} are the zonal and eddy available potential energy, respectively. T is temperature, p is pressure, g is acceleration of gravity, while u and v are zonal and meridional wind components, respectively. The vertical boundaries of integration are p_0 (pressure at the surface) and p_{TOP} (pressure at the top).

Conversions and transformations terms are given by

$$C\,(A_{\mathrm{Z}}, K_{\mathrm{Z}}) = -\int\limits_{p_{\mathrm{TOP}}}^{p_0} \frac{R}{gp} \overline{[\omega]''[T]''} \mathrm{d}p\,, \tag{5}$$

$$C\,(A_{\mathrm{Z}}, A_{\mathrm{E}}) = -\int\limits_{p_{\mathrm{TOP}}}^{p_0} \left\{ \overline{\frac{[T^*v^*]}{\sigma} \frac{\partial [T]''}{\partial y}} + \overline{\frac{[T^*\omega^*]}{p^{R/C_{\mathrm{P}}}} \frac{\partial}{\partial p} \left(\frac{[T]'' p^{R/C_{\mathrm{P}}}}{\sigma} \right)} \right\} \mathrm{d}p\,, \tag{6}$$

$$C\,(A_{\mathrm{E}}, K_{\mathrm{E}}) = -\int\limits_{p_{\mathrm{TOP}}}^{p_0} \frac{R}{gp} \overline{\omega^* T^*} \mathrm{d}p\,, \tag{7}$$

$$C\,(K_{\mathrm{Z}}, K_{\mathrm{E}}) = -\int\limits_{p_{\mathrm{TOP}}}^{p_0} \frac{1}{g} \left(\overline{[u^*v^*] \frac{\partial [u]}{\partial y}} + \overline{[v^{*2}] \frac{\partial [v]}{\partial y}} + \overline{[u^*\omega^*] \frac{\partial [u]}{\partial p}} + \overline{[v^*\omega^*] \frac{\partial [v]}{\partial p}} \right), \tag{8}$$

where ω is the vertical velocity in the isobaric coordinate system. In the above-mentioned equations, the symbol $C(X, Y)$ denotes the energy conversion (transformation) from X to Y.

Static stability (σ) is given by

$$\sigma = \frac{gT}{C_\mathrm{p}} - \frac{pg}{R}\frac{\partial T}{\partial p}\,, \tag{9}$$

where C_p is the specific heat of the air at constant pressure, and R is the gas constant for air.

When Lorenz's energy cycle is applied to an open area, then the transfer of kinetic and available potential energy across the boundaries has to be taken account [2]. The energy budget equations for a limited area are

$$\partial A_\mathrm{Z}/\partial t = -C(A_\mathrm{Z}, A_\mathrm{E}) - C(A_\mathrm{Z}, K_\mathrm{Z}) + G(A_\mathrm{Z}) + B(A_\mathrm{Z})\,, \tag{10}$$

$$\partial A_\mathrm{E}/\partial t = C(A_\mathrm{Z}, A_\mathrm{E}) - C(A_\mathrm{E}, K_\mathrm{E}) + G(A_\mathrm{E}) + B(A_\mathrm{E})\,, \tag{11}$$

$$\partial K_\mathrm{Z}/\partial t = C(A_\mathrm{Z}, K_\mathrm{Z}) - C(K_\mathrm{Z}, K_\mathrm{E}) - D(K_\mathrm{Z}) + B(K_\mathrm{Z}) + B(\Phi_\mathrm{Z})\,, \tag{12}$$

$$\partial K_\mathrm{E}/\partial t = C(A_\mathrm{E}, K_\mathrm{E}) - C(K_\mathrm{Z}, K_\mathrm{E}) - D(K_\mathrm{E}) + B(K_\mathrm{E}) + B(\Phi_\mathrm{E})\,, \tag{13}$$

where $B(A_\mathrm{Z})$, $B(A_\mathrm{E})$, $B(K_\mathrm{Z})$ and $B(K_\mathrm{E})$ are boundary energy fluxes of A_Z, A_E, K_Z and K_E, respectively. They are calculated according to

$$B\,(X) = -\frac{1}{g\,(x_2 - x_1)\,(y_2 - y_1)} \int\limits_p \int\limits_y \int\limits_x \left(\nabla_h \cdot X\vec{V}_h + \frac{\partial X\omega}{\partial p} \right) \mathrm{d}x\;\mathrm{d}y\;\mathrm{d}p\,; \tag{14}$$

$D(K_\mathrm{Z})$ and $D(K_\mathrm{E})$ denote the dissipation of K_Z and K_E, respectively. $B(\Phi_\mathrm{Z})$ and $B(\Phi_\mathrm{E})$ represent zonal and eddy boundary pressure work, respectively. Bearing in mind the known difficulties regarding the computation of these terms which give unrealistic values (see Brennan and Vincent [14]), they are combined with dissipation terms, $D(K_\mathrm{Z})$ and $D(K_\mathrm{E})$, as follows:

$$-R(K_\mathrm{Z}) = B(\Phi_\mathrm{Z}) - D(K_\mathrm{Z})\,, \tag{15}$$

$$-R(K_\mathrm{E}) = B(\Phi_\mathrm{E}) - D(K_\mathrm{E})\,. \tag{16}$$

These combined terms are computed as residuals. As a consequence it is quite difficult to interpret $R(K_\mathrm{Z})$ and $R(K_\mathrm{E})$ properly, since they involve boundary work, kinetic energy dissipation, any subgrid to grid scale transfer of K_Z and K_E, and also they contain errors accumulated during the numerical calculation of the other terms in eqs. (12) and (13). The generation terms of zonal and eddy available potential energy, $G(A_\mathrm{Z})$ and $G(A_\mathrm{E})$ respectively, are also estimated as residuals. Therefore they include accumulated error resulting from the numerical calculation of each of other terms in eqs. (10) and (11).

3. – Data and computation

Data set used in this study has been provided by ALADIN/LACE model developed at Météo France [15, 16]. The data refer to the period 18-21 November 1999 that was characterized by an intense cyclonic development over the Gulf of Genoa. A sub-domain inside ALADIN/LACE domain is defined so that the area under study encloses the

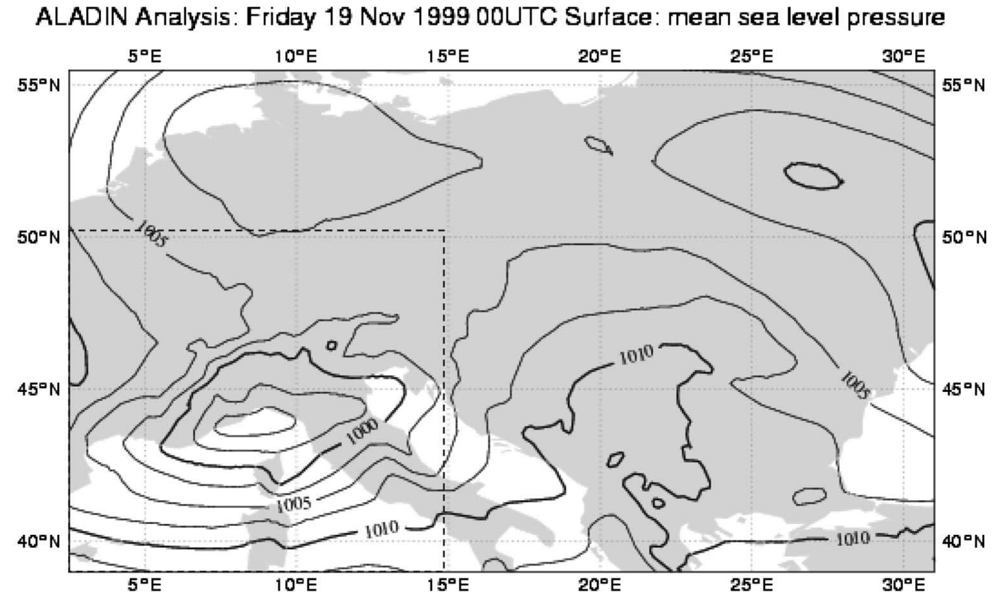

Fig. 1. – Sea-level pressure (hPa) on 19 November 1999 (00 UTC) over the ALADIN/LACE model domain. The area under study is delimited by a dashed line.

surface cyclone in such a manner that the cyclone is the major synoptic-scale disturbance there (fig. 1). A 100×100 horizontal grid with 12.176 km resolution has been used. The surface and the following higher isobaric levels (925, 850, 800, 700, 600, 500, 400, 350, 300, 250, 200, 100 and 50 hPa) have been considered. Data set consists of the wind components (u—zonal, v—meridional, ω—vertical), temperature (T) and surface pressure (p_0). Data are given twice a day, at 0000 UTC and 1200 UTC.

Derivatives were obtained by using the centred finite difference method. Integrations were performed in the vertical, from the surface to the 50-hPa isobaric level using the expanded trapezoidal rule.

4. – Synoptic conditions

The period 18-21 November 1999 is characterized by an intense cyclonic development over the Gulf of Genoa. Although the cyclone life cycle was relatively short, it strongly influenced meteorological conditions in the studied region and its rapid development was associated with severe weather conditions. Then, an unexpected copious snowfall occurred in Croatia.

The synoptic analysis on the surface level of 0000 UTC 18 November 1999 (fig. 2a) reveals a strong northerly airflow over the Alps. However, 12 hours later a low-pressure system (with the central pressure of 1005 hPa) had formed northwest from the Alps (fig. 2b). Simultaneously, geopotential troughs are present on the 300-hPa synoptic charts (fig. 3) and also on higher isobaric levels up to 100 hPa (not shown).

As shown in fig. 2c, during the next several hours the system passed over the Alps. Thus, at 0000 UTC 19 November 1999 the cyclone was located over the Gulf of Genoa. The pressure in its centre dropped down to 995 hPa. Holding the same central pressure,

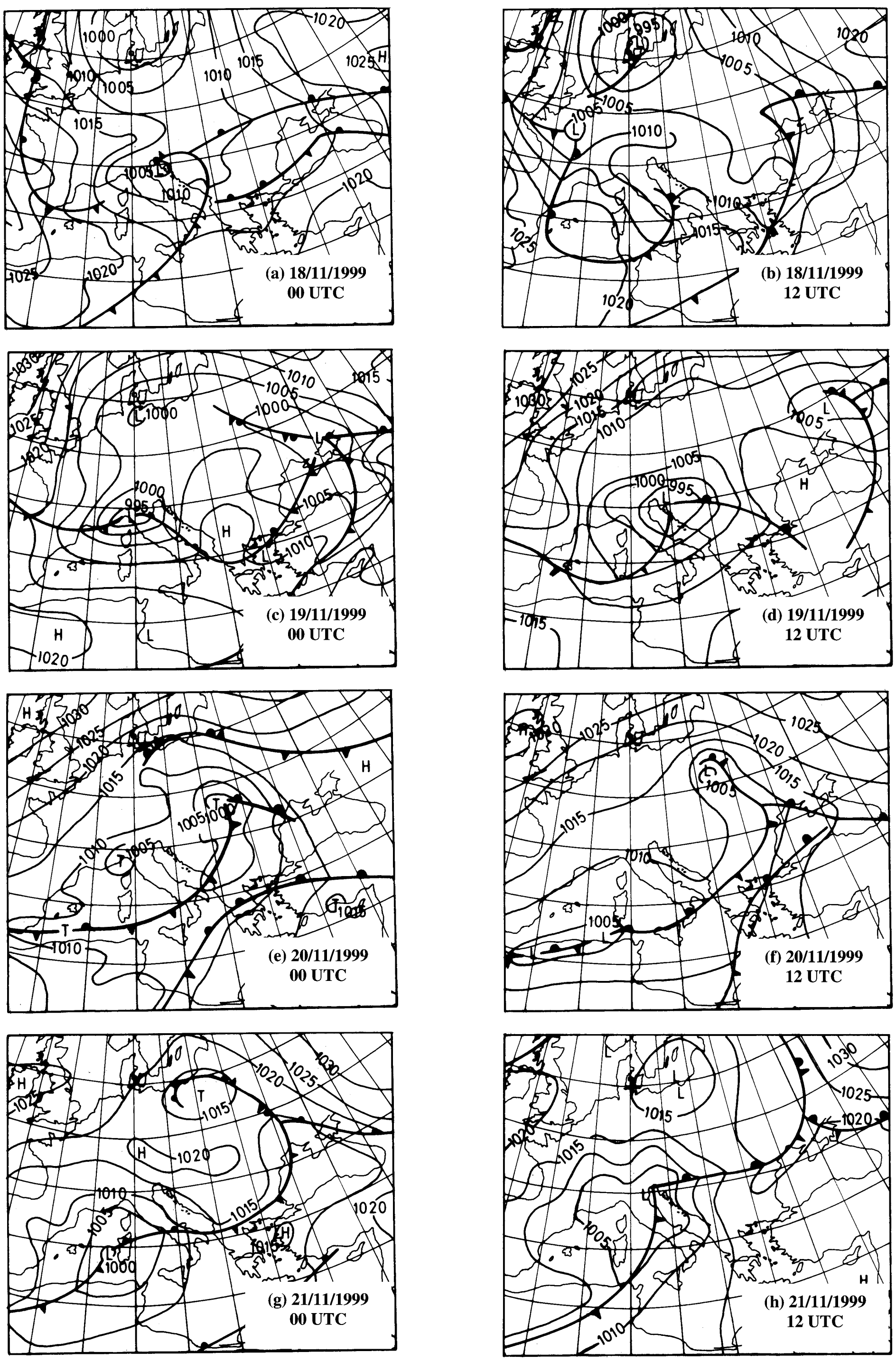

Fig. 2. – Surface synoptic charts: (a) 0000 UTC 18 Nov., (b) 1200 UTC 18 Nov., (c) 0000 UTC 19 Nov., (d) 1200 UTC 19 Nov., (e) 0000 UTC 20 Nov., (f) 1200 UTC 20 Nov., (g) 0000 UTC 21 Nov., (h) 1200 UTC 21 Nov. 1999.

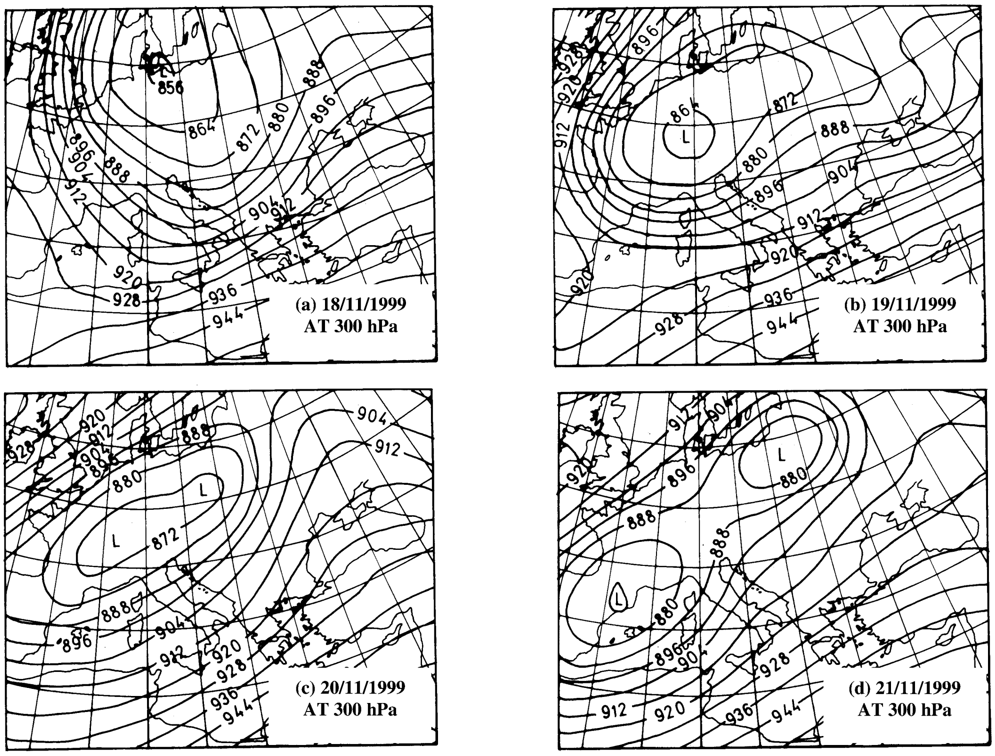

Fig. 3. – Absolute geopotential topography of 300-hPa isobaric level at 0000 UTC: (a) 18 Nov., (b) 19 Nov., (c) 20 Nov., (d) 21 Nov. 1999.

the cyclone was moving toward the east. So, 12 h later the system was placed over the north Adriatic Sea (fig. 2d). The intense development of the surface cyclone was accompanied by a low-pressure system with closed geopotential contours on the upper isobaric levels (not shown).

After the cyclone had reached its mature stage, it started to fill in. By 0000 UTC 20 November 1999, the cyclone had moved toward the northeast, while a low-pressure region remained in the lee of the Alps (fig. 2e). Further pressure filling continued in the next 12 hours, so low-pressure region was vanishing from the lee of the Alps (fig. 2f). However, on the synoptic charts of the upper isobaric levels the closed low was still present and underwent SW-NE stretching, and then split into two lows on 21 November 1999 (fig. 3).

The surface synoptic charts for 21 November 1999 (figs. 2g and 2h) do not contain any synoptic formation that could be connected with the studied cyclone. Thus, the life cycle of the studied cyclone was undoubtedly finished.

5. – Discussion of results

5·1. *Static stability.* – Figures 4 a-d illustrates the vertical distribution of horizontal area-averaged static stability parameter (eq. (9)) during the considered time period. Note two layers in the atmosphere with a pronounced vertical decrease of σ. The first one is in

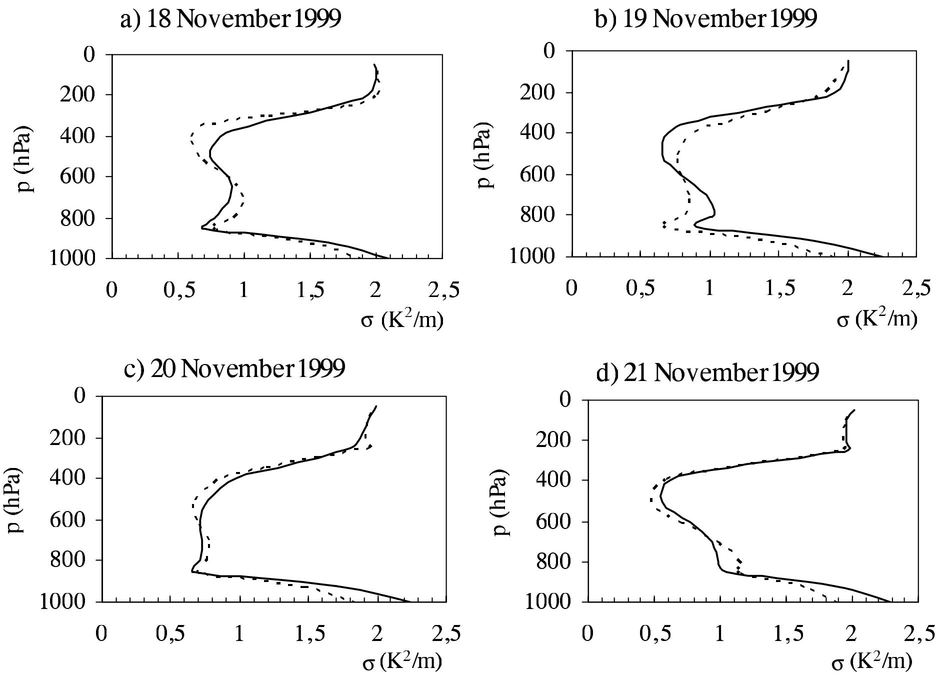

Fig. 4. – Vertical distribution of area-averaged static stability (σ) at 0000 UTC (bold line) and 1200 UTC (dashed line). Unit: (K^2/m).

the lower troposphere (1000–850 hPa) indicating less stable boundary layer. The other layer is located in the middle troposphere (700–400 hPa), so it seems reasonable to expect this layer to be more active in eddies than the others. In this layer, the most pronounced decrease of σ appears at 1200 UTC 18 November 1999 and 0000 UTC 19 November 1999. Thus, the period of σ-decrease coincides with intense cyclone development.

5˙2. *Vertical distribution of energy cycle components.* – Zonal and eddy components of area-averaged kinetic and available potential energy, their conversions and transformations are computed. They are presented in 12 h intervals during the time interval 18-21 November 1999, throughout the vertical layer from 1000 to 50 hPa. They are calculated and presented on considered isobaric levels as area-averaged values prior to vertical integration (*i.e.* as values of subintegral functions in eqs. (1)-(8)). The intention is to discuss the appearance of *main maximum* (the largest value of studied energy components considering the complete time period under the study and entire atmospheric depth) and also the appearance of *secondary maximum* (the largest value during the investigated time period, but at given isobaric surface), and their relation to the cyclone development. The vertical time section of A_Z is shown in fig. 5. It can be seen that A_Z alters on all the considered isobaric levels. The main maximum appears on the 500-hPa isobaric level on 19 November 1999. This coincides with the date of the mature stage of the studied cyclone (figs. 2 and 3). Secondary A_Z maxima on every investigated isobaric level below 500 hPa appear at the same time, on 19 November 1999. However, in the upper troposphere (above the 500-hPa isobaric level), a time-delay of individual secondary maximal values is evident. Such vertical distribution of A_Z indicates an up-

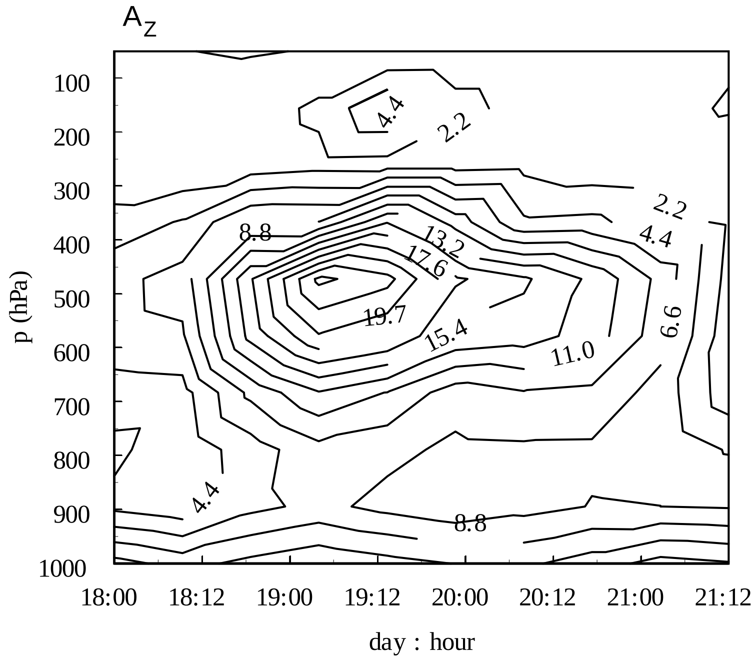

Fig. 5. – Vertical time section of zonal available potential energy A_Z. Date and time formats are dd:hh. Values are in $\mathrm{Jm^{-2}Pa^{-1}}$.

ward vertical energy transport from the lower and middle troposphere toward the upper levels. Furthermore, the most intense A_Z variations, both spatial and temporal, occur approximately on the 500-hPa isobaric level. This implies the baroclinity of this part of the atmosphere, and so upholds the aforementioned assumption about a strong eddy activity there.

A_E vertical time section (fig. 6) also represents spatial and temporal changeability with the most intense variations within the middle troposphere. The A_E main maximum shows up on the same level as A_Z, but 12 hours earlier (at 1200 UTC 18 November 1999 around 500 hPa). It is 3.5 times lesser than A_Z maximum. Secondary maximal A_E values on the isobaric levels between 500 and 300 hPa appear consecutively. Similarly as it has been concluded for A_Z, this indicates an upward A_E transport. In the lower troposphere (up to 500 hPa), intense cyclogenesis is preceded by an increase of A_E. Secondary maximal values in this part of the atmosphere appear at the same time, at 1200 UTC 18 November 1999. After that, A_E significantly decreases during the following 24 hours. Still, the lowest part of the troposphere (layer between the surface and the 850-hPa isobaric level) exhibits a noticeable increase in A_E starting from 1200 UTC 18 November 1999 to 1200 UTC 19 November 1999. Therefore, it seems reasonable to attribute this A_E increment to energy conditions that are favourable to the maintenance of the surface cyclone. However, the significant weakening of the cyclone is evident on surface synoptic charts on 20 November 1999 (fig. 2e). Though this seems contradictory at first sight, it may also implicate the presence of some destructive mechanism that does not allow further existence of the cyclone. Moreover, it is well known that trough axes tilt may indicate attenuation or maintenance of disturbance development in quasy-geostrophic

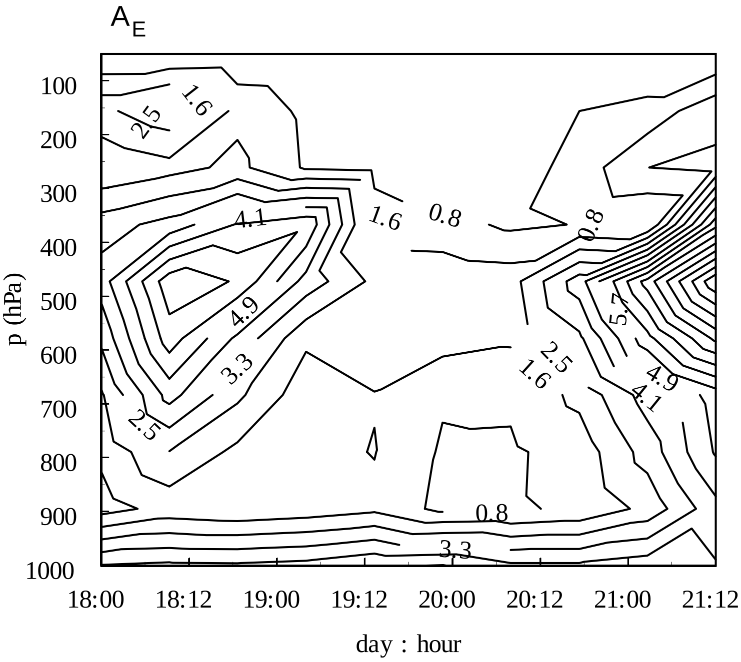

Fig. 6. – Vertical time section of eddy available potential energy A_E. Date and time formats are dd:hh. Values are in $\mathrm{Jm}^{-2}\mathrm{Pa}^{-1}$.

atmosphere [17]. Thus, phase relationship between troughs at 500 hPa and 1000 hPa, which causes vertical axes to be tilted toward the west, indicates that divergence in the middle troposphere supports the surface convergence and, consequently, the wave amplification. On the other hand, the vertical axis that is tilted toward the east is related to the attenuation of disturbance development. Therefore, it seems logical to assume the following tentative development of the disturbance: the studied cyclone was placed over the Gulf of Genoa at 0000 UTC 19 November 1999 (fig. 2c), and it was accompanied by favourable surface energy conditions (A_E generation). However, the closed system on the 500-hPa isobaric level had moved toward the east (not shown), and thus caused a significant eastward axis tilt with height, which resulted in dynamically unfavourable conditions for further development on the surface. Consequently, the filling of the surface cyclone occurred.

Zonal kinetic energy (fig. 7) strengthens significantly with height. The maximal amounts, which are concentrated around the 250-hPa isobaric level, are caused by a jet stream. Both the jet stream and K_Z have the greatest amounts on 19 and 20 November 1999. In general, during the investigated time period, maximal K_Z values appear in the layer from 350 to 150 hPa. Synoptic charts also indicate strong horizontal wind gradients on the same levels. Thus, pronounced vertical and horizontal wind shears characterize this part of the atmosphere. As one may see in the 850–250 hPa layer, K_Z slightly increases at the beginning of the time period, and slightly decreases after 0000 UTC 19 November 1999.

Similar to K_Z, eddy kinetic energy has increased values within the upper troposphere (fig. 8). Main K_E maximum is found at 0000 UTC 19 November 1999 around the 300-hPa

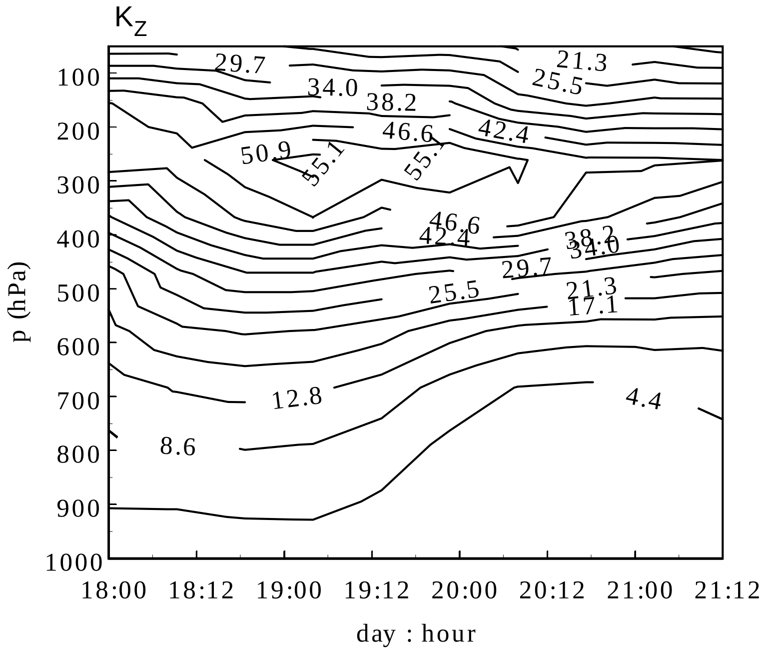

Fig. 7. – Vertical time section of zonal kinetic energy K_Z. Date and time formats are dd:hh. Values are in $Jm^{-2}Pa^{-1}$.

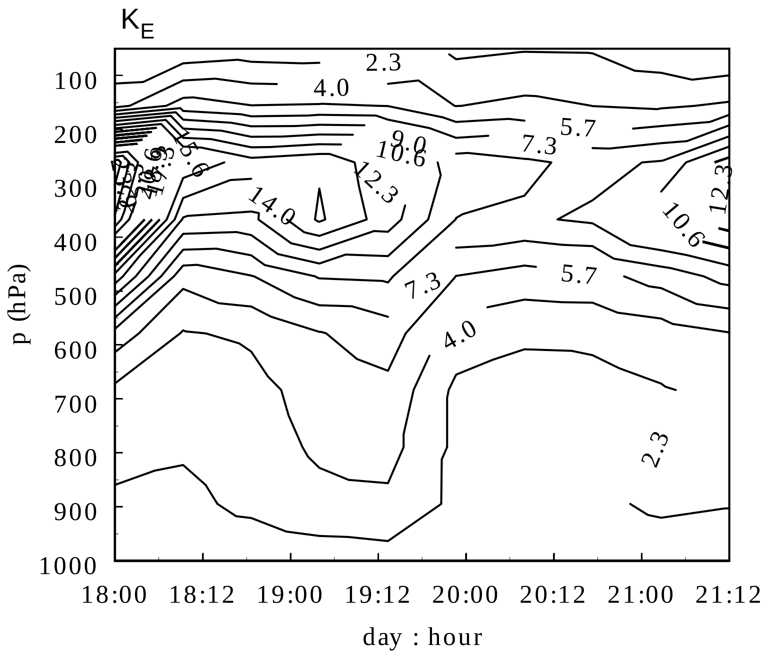

Fig. 8. – Vertical time section of eddy kinetic energy K_E. Date and time formats are dd:hh. Values are in $Jm^{-2}Pa^{-1}$.

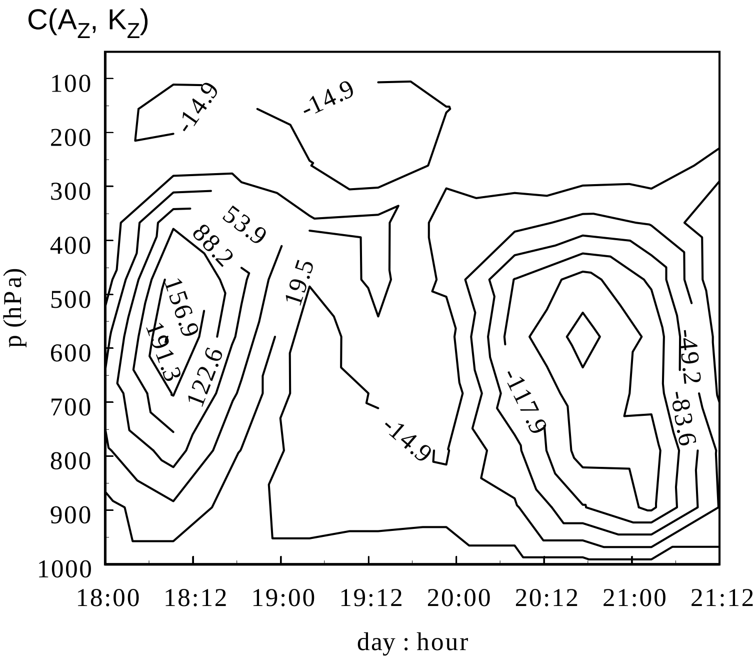

Fig. 9. – Vertical time section of transformation $C(A_{\mathrm{Z}}, K_{\mathrm{Z}})$. Date and time formats are dd:hh. Values are in 10^{-5} $\mathrm{Wm}^{-2}\mathrm{Pa}^{-1}$.

isobaric level. It can be inferred that the vortex is formed in the upper troposphere and is the most intense there. Note that isobaric levels from the surface to 400 hPa exhibit individual maximum values with certain time shifts (*i.e.* K_{E} maximum shows a downward shift with time). Such a behaviour indicates downward K_{E} transport. Surface K_E maximum appears at 1200 UTC 19 November 1999, exactly when the surface cyclone is the most intense, and so is its circulation. As K_{E} maximums decrease toward the ground, it is obvious that the cyclone also becomes dynamically weaker in this direction (*i.e.* eddy motion weakens). Compared to A_{E}, energy of eddy motion, K_{E}, shows greater values than A_{E} through the whole deepness of the atmosphere, except in its lowest part, *i.e.* near the ground. This domination of A_{E} over K_{E} is more pronounced during the existence of the surface cyclone.

All of the energy forms are physically related to transformation and conversion processes (eqs. (5)-(8)). Note the different behaviour of $C(A_{\mathrm{Z}}, K_{\mathrm{Z}})$ in the layers above and under 300 hPa (fig. 9). The prevalent negative sign of $C(A_{\mathrm{Z}}, K_{\mathrm{Z}})$ above the 300-hPa level indicates a stratospheric energy regime with K_{Z} acting as a source of A_{Z}. In contrast, $C(A_{\mathrm{Z}},K_{\mathrm{Z}})$ exhibits an oscillatory character within the troposphere. Thus, A_{Z} acts as a significant source of K_{Z} at the beginning of the cyclone development. The most intense transformation occurs at 1200 UTC 18 November 1999 simultaneously on all the tropospheric levels (leading to the surface cyclone development). After the cyclone has developed, at 0000 UTC 19 November 1999, $C(A_{\mathrm{Z}},K_{\mathrm{Z}})$ changes the sign. Consequently, A_{Z} retrieves energy back from K_{Z}. Note that the maximal values of this process (in both directions) again take place within the 600–500 hPa layer.

During the first stages of the cyclone development, the negative conversion term

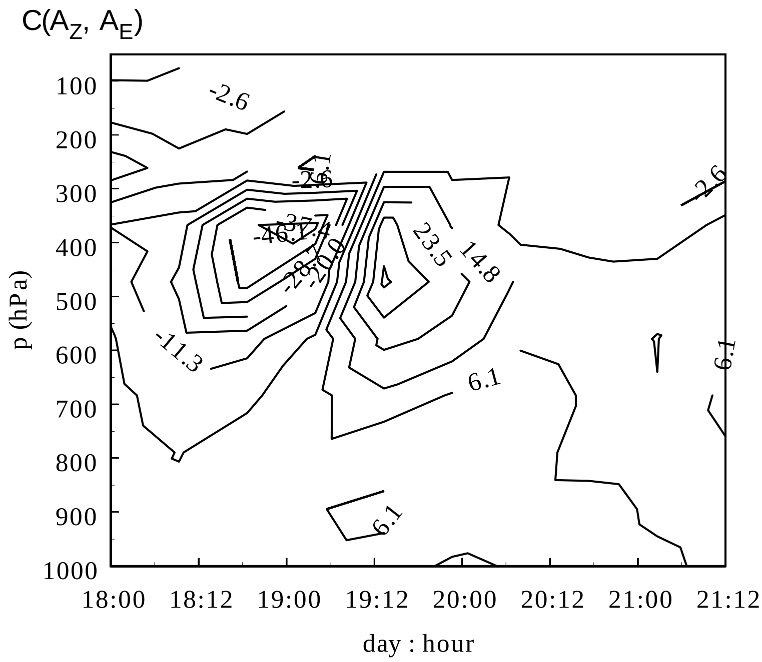

Fig. 10. – Vertical time section of conversion $C(A_\mathrm{Z},\, A_\mathrm{E})$. Date and time formats are dd:hh. Values are in 10^{-5} $\mathrm{Wm^{-2}Pa^{-1}}$.

$C(A_\mathrm{Z},\, A_\mathrm{E})$ indicates A_E to be the source of A_Z (fig. 10). Thus, A_Z receives the energy from A_E and transfers it to K_Z. Following the mature stage of the cyclone (19 November 1999), the conversion $C(A_\mathrm{Z},\, A_\mathrm{E})$ has a positive sign, and so A_Z acts as the source of A_E. The most intensive conversions are again within the midtroposphere. Note the secondary maximum of A_Z to A_E conversion in the lower troposphere at 12 UTC 19 November 1999. It coincides with the secondary maximum of A_E in the same part of the troposphere (fig. 6). Thus, conversion from A_Z to A_E is the process that maintains further surface cyclone development. However, it is insufficient compared with the processes caused by the above-mentioned eastward axis tilt and related attenuation.

A positive rate of conversion from A_E to K_E represents a measure of baroclinic cyclogenesis (the process of warm air rising and cold air sinking at the same latitude). But, in this study the transformation $C(A_\mathrm{E}, K_\mathrm{E})$ mainly maintains a negative value (fig. 11). One may see a positive transformation in the upper layer, with its maximum reached at 0000 UTC 19 November 1999 at 350 hPa. Certainly, this process contributes to the K_E increment in this part of the atmosphere (fig. 8). However, the negative sign of this process (which represents a sink of K_E) dominates over the time and space. The most pronounced $A_\mathrm{E} \rightarrow K_\mathrm{E}$ transformation is again within the 600–500 hPa layer (the same as already mentioned $C(A_\mathrm{Z},\, A_\mathrm{E})$ and $C(A_\mathrm{Z},\, K_\mathrm{Z})$ processes). The transformation process is very intense at 1200 UTC 19 November 1999 through the whole troposphere. Furthermore, the sign and amount of this term indicate a copious loss of K_E. In spite of that, K_E increases through the whole atmosphere at the same time (fig. 8), and it is evident that it is not the consequence of $C(A_\mathrm{E}, K_\mathrm{E})$ transformation. Thus, some other plentiful energy source for K_E must exist.

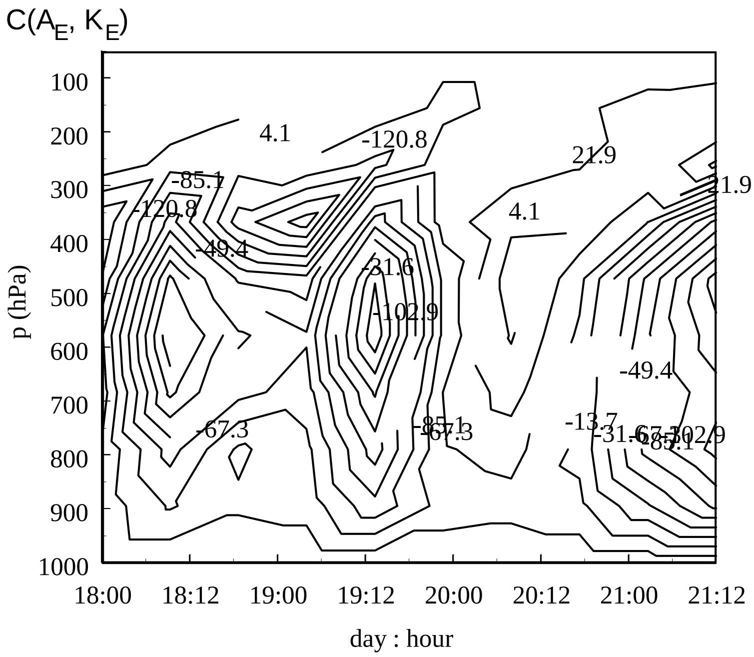

Fig. 11. – Vertical time section of transformation $C(A_{\mathrm{E}}, K_{\mathrm{E}})$. Date and time formats are dd:hh. Values are in 10^{-5} $\mathrm{Wm^{-2}Pa^{-1}}$.

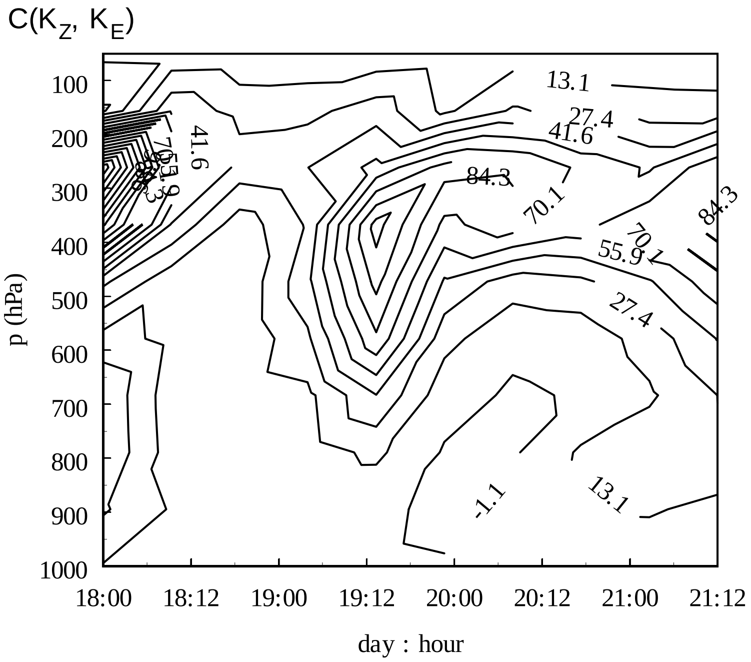

Fig. 12. – Vertical time section of conversion $C(K_{\mathrm{Z}}, K_{\mathrm{E}})$. Date and time formats are dd:hh. Values are in 10^{-5} $\mathrm{Wm^{-2}Pa^{-1}}$.

As can be seen in fig. 12, K_{E} gains energy from K_{Z} due to the conversion $C(K_{\mathrm{Z}}, K_{\mathrm{E}})$ processes. Since $C(K_{\mathrm{Z}}, K_{\mathrm{E}})$ depends on vertical and horizontal wind shears (eq. (8)), it does not seem surprising that the most intense conversion takes place within the 400–300 hPa layer. The analysis of vertical distribution of K_{Z} (fig. 7) has already pointed out quite large wind shears in this atmospheric layer. At 1200 UTC 19 November 1999 all layers from the surface to 350 hPa gain maximal $C(K_{\mathrm{Z}}, K_{\mathrm{E}})$ values. However, layers above 350 hPa exhibit maximal conversion with the time delay. One may see longer duration of intensive conversion in that part of the atmosphere, which is in accordance with longer lifetime of disturbance there. It is obvious that the zonal flow feeds the disturbance in all the layers above 800 hPa. This is a reverse process to what normally happens in the general circulation, where zonal flow is maintained by supplying kinetic energy from synoptic disturbances.

According to the aforesaid discussion, both K_{Z} and K_{E} and their conversion have a crucial role in the studied cyclone development. Furthermore, barotropic energy conversion $C(K_{\mathrm{Z}}, K_{\mathrm{E}})$ is connected with the vortex formation in the upper atmosphere. As the other energy cycle components do not reflect the formation of the cyclone, it presents the main mechanism of the cyclone evolution during the whole lifetime of the cyclone. After the cyclone formation, both $C(K_{\mathrm{Z}}, K_{\mathrm{E}})$ and $C(A_{\mathrm{Z}}, A_{\mathrm{E}})$ maintain the cyclone, but $C(K_{\mathrm{Z}}, K_{\mathrm{E}})$ is undoubtedly a dominant process. The comparison between the results obtained by Mishra and Rao [18] and this study indicates that a life cycle of cyclonic vortex over Brazil and the examined Genoa cyclone have some similarities in spite of their different geographical positions. Thus, the formation of both, the studied Genoa cyclone and the cyclonic vortex over Brazil is maintained by energy conversion from K_{Z} to K_{E}. Furthermore, the process responsible for formation of the vortex over Brazil was also located in the upper layer of the atmosphere, and a strong shear zone preceded its development. Still, the vortex over Brazil was confined to the upper troposphere. On the contrary, the vortex formed in the upper atmosphere under this study reached the ground over the Gulf of Genoa thanks to plentiful energy transport and stability conditions of the middle atmosphere that have allowed the transport.

As can be seen in fig. 13, vertical profiles of K_{Z} and K_{E} have the expected shape. They increase with height, *i.e.* from the surface to the peak level (300–250 hPa). K_{Z} exceeds K_{E} on all levels. Direct attention to variations of kinetic energy at 300 hPa: K_{Z} increases more or less gradually from 43.9 $\mathrm{J/(m^2Pa)}$ at 0000 UTC 18 November 1999 to 59.3 $\mathrm{J/(m^2Pa)}$ at 0000 UTC 19 November 1999. On the contrary, K_{E} sharply decreases from 33.9 $\mathrm{J/(m^2Pa)}$ at 0000 UTC 18 November 1999 to 11.1 $\mathrm{J/(m^2Pa)}$ at 0000 UTC (approximately three times in 12 hours). During the following 12 hours, it increases to 18.2 $\mathrm{J/(m^2Pa)}$. At the same time, synoptic charts indicate strengthening of the closed system at 300 hPa. Nevertheless, eddy kinetic energy decreases in spite of the cyclonic development. This seems surprising because the cyclone reaches its mature stage on 19 November 1999, so a simultaneous strong cyclonic flow (and consequently an increase of K_{E}) is expected. Furthermore, conversion $C(K_{\mathrm{Z}}, K_{\mathrm{E}})$ is both positive and large. Thus, the expected result would reflect strong eddy motion and an appreciable increase of K_{E}. For an explanation of the mentioned result for K_{Z} and K_{E}, see the 300-hPa synoptic charts (fig. 3). Obviously, the closed system exists on 18 November 1999 on the 300-hPa isobaric level, but its centre is outside the area under study. In the next 24 hours, the system moves toward the southeast. Geopotential gradient implies that cyclonic flow strengthens, so an enlargement of K_{E} is expected. However, the southern part of the system (which is placed over the area under study) has isopleths that coincide with geographical parallels. In other words, wind is east-west oriented in this part of

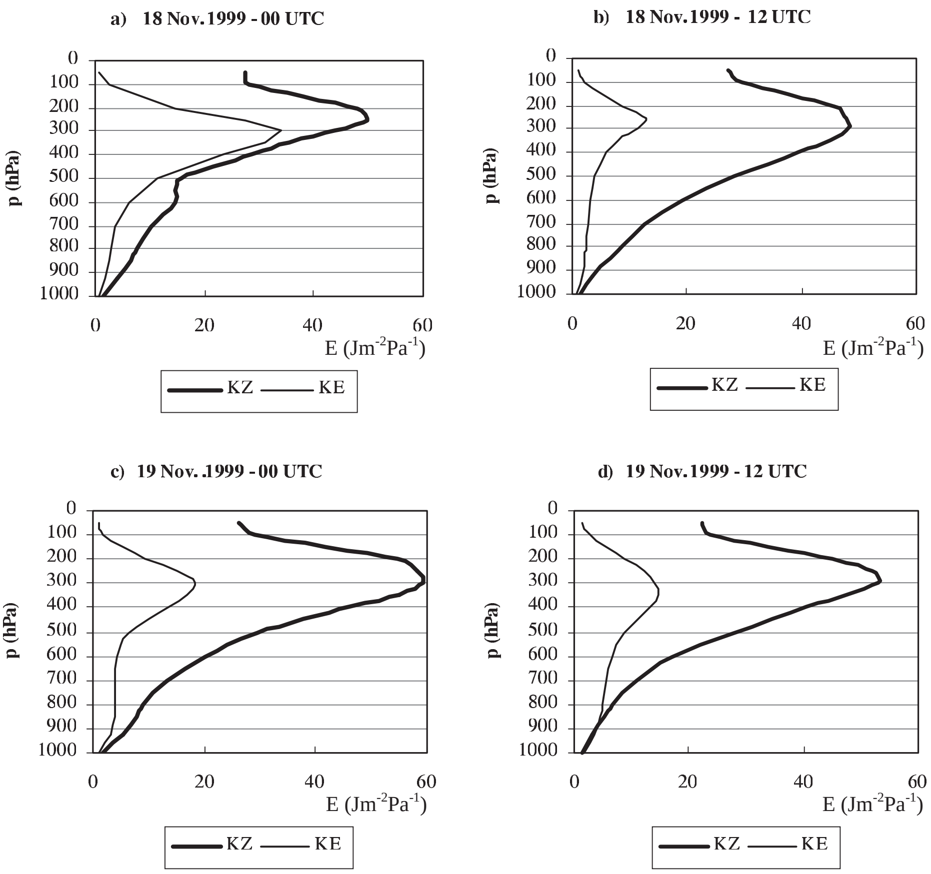

Fig. 13. – Vertical distribution of zonal and eddy kinetic energy. Values are in $\mathrm{Jm^{-2}Pa^{-1}}$.

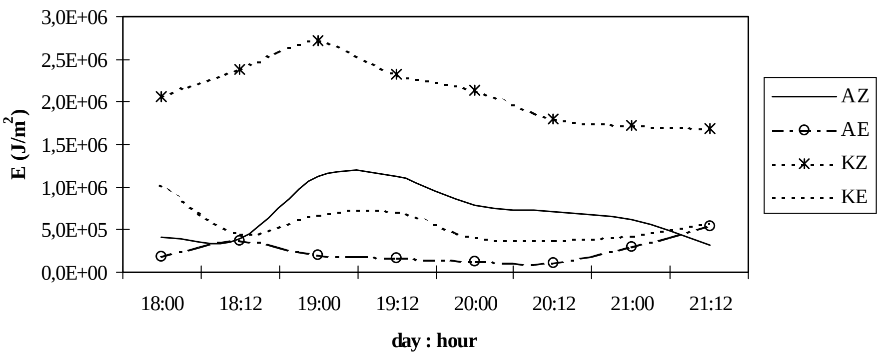

Fig. 14. – Energy contents during the time period 18-21 Nov. 1999.

disturbance. The model used to calculate the energy cycle attributes wind speeds in this part of the atmosphere to zonal flow instead to eddy flow. Consequently, there is a strong zonal component, so the obtained K_{Z} sharply increases. Therefore, this is the result of the relation between the horizontal domain of the model and the shape and size of upper disturbance. This problem is present only at 300 hPa (compare figs. 14a and 14c). On the lower levels (below 700 hPa), there is a cyclone growth accompanied by a K_{E} increment. Due to air density reduction, the cross-section of the cyclonal vortex is extended by height, so the horizontal domain of the model contains only a part of the system on the upper levels. To avoid this problem, the enlargement of the horizontal domain should be employed. In this case, however, a problem would turn up in the lower part of the atmosphere. The horizontal domain of the model fitted to the size of the upper system, would cover not only the studied cyclone, but also other synoptic systems that lie around on the surface level. As a result of this, energy cycle components would reflect the influence of all the adjacent synoptic systems together. Consequently, the impact of the studied cyclone on the energetics calculations would be disguised, especially in the lower atmosphere. A preliminary calculation of energy budget over some larger sub-domains as well as over the whole domain of ALADIN/LACE model showed that results do not demonstrate the expected influence of the studied cyclone (not presented here). For example, results calculated over the whole ALADIN/LACE domain indicated an amount of eddy kinetic energy which is the lowest when the intensity of the surface low is the largest (19 November 1999). Furthermore, the sum of conversion $C(K_{\mathrm{Z}}, K_{\mathrm{E}})$ and transformation $C(A_{\mathrm{E}}, K_{\mathrm{E}})$ is negative throughout the cyclogenesis, which contradict the expectations. In that case, the energy budget can be examined as a contribution of that volume to the energy budget of the whole atmosphere, while the effect of the particular disturbance is masked. This shows that an enlargement of computational area does not necessary improve results and their interpretation.

5˙3. *Volume-integrated components of energy cycle.* – Zonal and eddy components of kinetic and available potential energy, as well as their conversions and transformations are calculated in 12-h intervals for each of the 14 vertical levels as area average values. Volume-integrated components are obtained by integrating over the entire volume over the computational area. Time variations of volume-integrated zonal and eddy parts of kinetic and available potential energy are shown in fig. 14. The dominance of K_{Z} within the studied atmospheric volume is evident. It exceeds the sum of the remaining energy forms. During the first day, K_{Z} shows a considerable increase due to the above-mentioned situation at 300-hPa (geographical position of cyclonic system and horizontal domain of the model). Due to this situation the impact of K_{Z} increase at 300 hPa level is so strong that it has also caused a pronounced increase of volume-integrated K_{Z} (fig. 14). The onset of the surface cyclogenesis is marked by an increase in K_{E} after 1200 UTC 18 November 1999. K_{E} increases rapidly during the next 12 h, so on the day of vortex formation K_{E} shows a large gain, of approximately 54%, from its value on the previous day. Next 12 h K_{E} increases very slightly (only 5%). After 1200 UTC 19 November 1999, the cyclone weakens and so does the eddy motion, thus K_{E} decreases rapidly.

A_{Z} is larger than A_{E} during the cyclone life cycle (fig. 14). Its maximum coincides with the mature stage of the cyclone. Zonal available energy depends on the distribution of zonally averaged temperature (eq. (1)). Thus, it is expected that powerful differential heating causes a copious quantity of A_{Z}. Land-sea thermal effect may have a crucial impact on the cyclone development. In this case study, the Gulf of Genoa in the southern part of the domain represents a relatively warm area compared to the cold flow from the

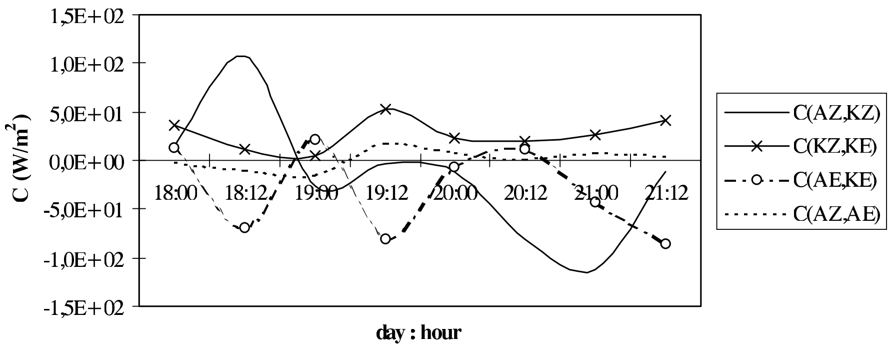

Fig. 15. – Energy transformation and conversion terms during the time period 18-21 Nov. 1999.

northwest. As the flow is approaching the Alps, meridional thermal gradient is increasing. Consequently, A_{Z} also increases (as can be seen in fig. 14). Theoretically, the land-sea thermal effect is expected to have some influence on A_{E}, because it may cause a deviation from the zonally arranged temperature field (*i.e.* the field due to differential heating of the Earth). However, fig. 14 clearly shows that A_{E} first increases at the beginning of the considered period. Later, it is slowly decreasing after 18 November 1999. Thus, the maximal A_{E} value appears during the precyclogenetic period. The illustrated behaviour of A_{Z} and A_{E} is a consequence of the geographical position of the Gulf of Genoa and the Alps in relation to the limited area under the study. The Gulf of Genoa and cold air behind the Alps represent warm and cold temperature sources respectively, and they are oriented south-north. Thus, they induce both the strengthening of zonal temperature differences in meridian direction and the increase of A_{Z}.

According to the synoptic charts, the cyclone under study is the most intense on 19 November 1999 that coincides with maximal K_{E} on that day. This is reasonable because the intensification of the disturbance is accompanied by strengthening of its eddy motion, leading to the K_{E} increase. The aforementioned discussion implies that the limited area energetics estimated in this study is basically dominated by the formation of the embodied system. Furthermore, it needs emphasizing that interpretation of the results has to include the geographical position of the cyclone in relation to the model domain.

The precyclogenetic period is signified by an intense transformation of A_{Z} to K_{Z} (fig. 15). This process increases rapidly during the first 12 hours. The transformation between A_{Z} and K_{Z} changes direction then. $C(A_{\mathrm{Z}}, K_{\mathrm{Z}})$ is already negative at 0000 UTC 19 November 1999, and holds the same sign till the end of the considered time period. Therefore, it is an important sink of K_{Z}. The energy conversion which includes eddy transport of sensible heat is represented by term $C(A_{\mathrm{Z}}, A_{\mathrm{E}})$. It is negative during the first 36 hours, but it changes direction after the cyclogenesis onset. It seems that this process does not have any significant role for the cyclone formation in the studied case because the direction of this conversion does not present the source of eddy energy during the cyclogenetic period. The direction of transformation represented by the term $C(A_{\mathrm{E}}, K_{\mathrm{E}})$ is changeable. During the precyclogenetic period, transformation is directed from K_{E} to A_{E}. As the surface cyclone is being formed, it changes direction. Thus $C(A_{\mathrm{E}}, K_{\mathrm{E}})$ contributes to K_{E} enhancement, which is noticeable at 0000 UTC 19 November 1999 (fig. 14). The barotropic conversion term, $C(K_{\mathrm{Z}}, K_{\mathrm{E}})$, is the only term with unchanging

TABLE I. – *Time averages of vertically integrated energy contents, energy conversions and transformations and sum of all energy forms (E) over the Gulf of Genoa for time period 18-21 Nov. 1999 and yearly averaged components of energy cycle over Northern hemisphere (from* [19]*). Energy units are in* $10^5 J/m^2$*; energy transformation and conversion units are in* Wm^{-2}.

	Genoa cyclone 18-21 November 1999	Northern hemisphere
A_Z	6.9	33.5
K_Z	21.6	3.6
A_E	2.5	15.6
K_E	5.9	8.8
$C(A_Z, K_Z)$	−15.8	−0.2
$C(K_Z, K_E)$	27.1	−0.3
$C(A_E, K_E)$	−29.9	2.2
$C(A_Z, A_E)$	2.1	1.5

sign. It is positive throughout the whole time period. So, it represents a copious source of K_E. Maximal conversion occurs at 1200 UTC 19 November 1999. Obviously, the formation of this cyclone is characterized by an intense conversion of kinetic energy from the zonal flow. During the first day of the considered period, the A_Z acts as a strong source of K_Z. Later, K_Z feeds the eddy motion. The cyclone formation is accompanied by the positive value of $C(A_E, K_E)$, but after 0000 19 November 1999 $C(K_Z, K_E)$ has a major role in the formation and intensification of the disturbance.

Overall quantities of energy contents, transformations and conversions (obtained here from vertically integrated time-averaged energy components during the cyclone development) are presented in table I. Both conversions from zonal to eddy energy, $C(A_Z, A_E)$ and $C(K_Z, K_E)$, are positive. As the result of this, zonal energy forms appear as sources of eddy forms. The comparison of results presented in this work and values for the Northern Hemisphere adopted from Oort and Peixoto [19] confirms the differences between the energetic processes influenced by individual synoptic systems and the energy cycle of the whole hemisphere. The energy components obtained in this study differ from the Northern Hemisphere not only in the amounts of energy components, but also in the direction of energy cycle. It is well known that the general circulation is maintained by eddies which supply kinetic energy to the zonal flow. On the contrary, in this study, the sign of $C(K_Z, K_E)$ conversion is positive during the entire investigated period, resulting in so intensive horizontal and vertical shear of the zonal wind that it acts as the vortex trigger. Further, K_E is greater than A_E during the cyclone period (figs. 7, 9 and 15), so it can be inferred that the dynamical characteristics of the system are more pronounced than the thermal ones. These results are in agreement with Alpert *et al.* [10] who suggests that the sea thermal effect, which is associated with the sea surface temperature, gives a considerable contribution to cyclogenesis in the Gulf of Genoa only during the summer months. The results of this case study also indicate that the investigated cyclone (which developed in the cold part of year) was extremely dependent on wind shear and conversion $C(K_Z, K_E)$. On the other hand, the thermal effect did not have a noticeable influence on its development. Certainly, to confirm this conclusion more energetics analyses of winter, as well as summer cyclones, are necessary.

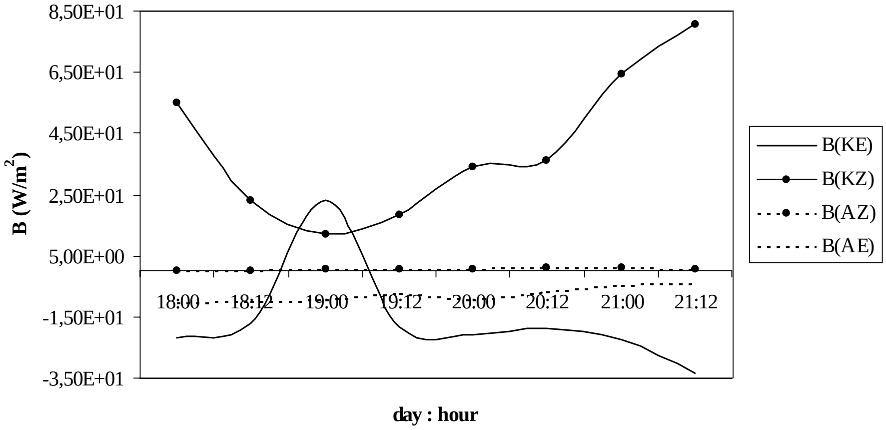

Fig. 16. – Boundary energy transfers during the time period 18-21 Nov. 1999.

5·4. *Boundary energy transfers and residues.* – Figure 16 shows integrated boundary energy transfers, *i.e.* $B(K_\mathrm{Z})$, $B(K_\mathrm{E})$, $B(A_\mathrm{Z})$, and $B(A_\mathrm{E})$ over the computational area. According to the formulation in eqs. (10)-(13), a positive value of energy flux indicates a transfer of corresponding energy form into the area under the study from the surrounding area (an energy import), while a negative value indicates a transfer from the area under study to the surrounding area (an energy export).

During the whole investigated period, there exists a large import of K_Z into the area under study. Compared with other boundary fluxes, $B(K_\mathrm{Z})$ presents a major energy transfer during the considered time period, except for the 0000 UTC 19 November 1999 when $B(K_\mathrm{E})$ is dominant. Considering all eight times together, the mean import K_Z rate is 40.7 Wm^{-2}. Unlike $B(K_\mathrm{Z})$, the transport of eddy kinetic energy, $B(K_\mathrm{E})$, maintains a negative value during the considered period, except for the 0000 UTC 19 November 1999 when this transfer reverses its direction. This large import of K_E coincides with cyclone formation. Overall, the K_E is exported from the computational area at a mean rate of 16.1 Wm^{-2}. $B(A_\mathrm{Z})$ maintains the lowest profile compared with the other three boundary fluxes, but it represents a continuous energy import to the area under the study. The mean rate of this transfer is 0.69 Wm^{-2}. The rate of A_E transfer, $B(A_\mathrm{E})$ represents continuous export of A_E from the computational area with the mean rate of 7.6 Wm^{-2}.

Regarding the behaviour of boundary energy transfers, it could be concluded that both zonal energy forms, K_Z and A_Z, are imported into the area under study during the investigated time period. Contrary, the eddy energy forms, K_E and A_E, are exported out of the limited area. The only exception is 0000 UTC 19 November 1999, when a large amount of K_E (23 Wm^{-2}) is imported.

Generation terms, $G(A_\mathrm{Z})$ and $G(A_\mathrm{E})$, are computed as the residuals from eqs. (10) and (11), respectively. Thus they not only represent generation due to diabatic heating processes, but in addition they also contain errors accumulated during the computation. In order to evaluate the residuals it is necessary to calculate tendencies of A_Z and A_E. Since ALADIN/LACE model is run twice a day, this represents a coarse temporal resolution of the available analysis data for such kind of calculations. Consequently, the evaluation of the residuals is problematic here, so the results obtained as residuals

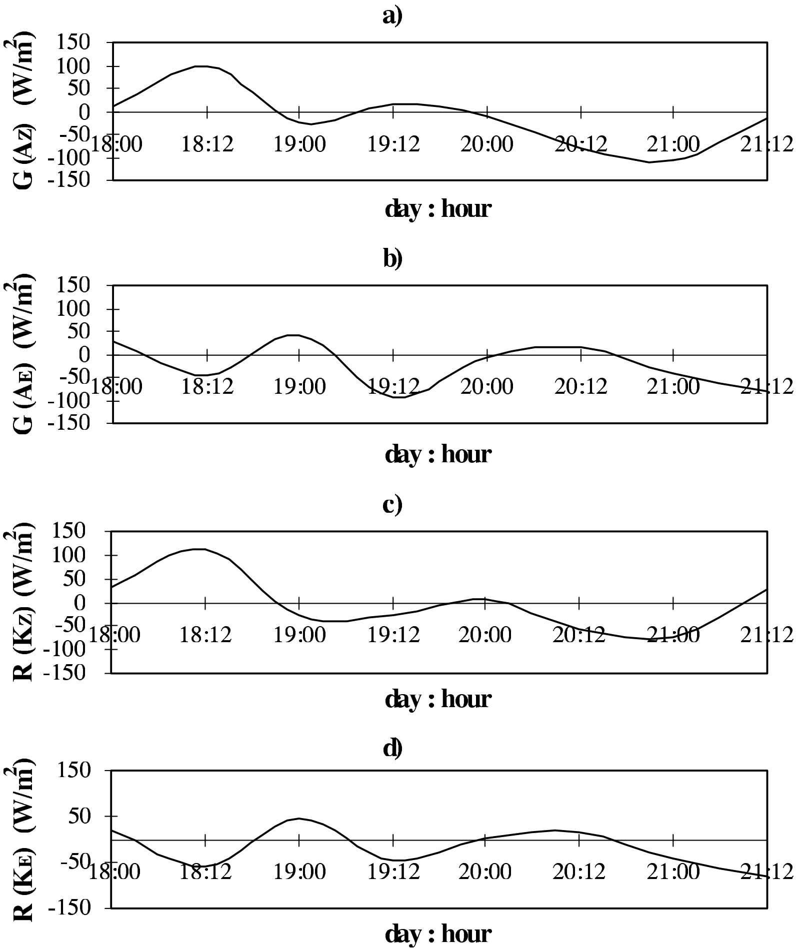

Fig. 17. – Residue terms $R(K_\mathrm{Z})$ and $R(K_\mathrm{E})$ and the generation terms $G(A_\mathrm{Z})$ and $G(A_\mathrm{E})$ during the time period 18-21 Nov. 1999.

should be considered rather as rough estimations. At the beginning of the time period, $G(A_\mathrm{Z})$ contribute to a large gain of A_Z (fig. 17 a), and it is much larger than import of this form of energy by boundary energy transfer $B(A_\mathrm{Z})$. A comparison of the terms $C(A_\mathrm{Z}, K_\mathrm{Z})$ and $C(A_\mathrm{Z}, K_\mathrm{E})$ in fig. 15 and also with $B(A_\mathrm{Z})$ in fig. 16, indicates that the increase of A_Z noticeable in fig. 14 from the 1200 UTC 18 November to the 0000 UTC 19 November 1999 can be attributed to its generation due to $G(A_\mathrm{Z})$ term. After 0000 UTC 19 November, $G(A_\mathrm{Z})$ is mainly negative (except the 1200 UTC 19 November when it has a relative small positive value), so it contributes to the A_Z decrease seen in fig. 14.

According to fig. 17 b, $G(A_\mathrm{E})$ has the maximal positive value at 0000 UTC 19 November. But, as has already been mentioned, A_E achieves its maximal value at 1200 UTC 18 November and monotonically decreases afterwards (see fig. 15). Furthermore, the strong increase in A_E at the beginning of period cannot be attributed to the boundary flux term $B(A_\mathrm{E})$, since it is negative through the whole period. The conversion from A_Z to A_E is negative then, so it represents A_E loss (see $C(A_\mathrm{Z}, A_\mathrm{E})$ in fig. 15). Hence, it seems that the increase of A_{E} is basically due to its gain from $C(A_{\mathrm{E}}, K_{\mathrm{E}})$.

Time variation of $G(A_{\mathrm{E}})$ shows that the generation of A_{E} is negative during the cyclogenetic period and it changes the sign on 0000 UTC 19 November when the cyclone is already formed. The conversion $C(A_{\mathrm{Z}}, A_{\mathrm{E}})$ is also negative. However, K_{E} and $C(K_{\mathrm{Z}}, K_{\mathrm{E}})$ accompany the cyclone formation. Considering this together with the vertical distribution of K_{Z}, K_{E} and $C(K_{\mathrm{Z}}, K_{\mathrm{E}})$ discussed earlier, it can be inferred that the cyclone development is dynamically conditioned rather than thermally. Furthermore, as K_{E} is greater than A_{E} (more than twice in average), it seems that the cyclone is a dynamically stronger and thermally weaker disturbance.

$R(K_{\mathrm{Z}})$ and $R(K_{\mathrm{E}})$ are presented in figs. 17c and 17d. It can be seen that $R(K_{\mathrm{Z}})$ first acts as a sink of K_{Z}, and after 0000 UTC 19 November it acts mostly as a source of K_{Z}. It is expected that frictional processes dissipate kinetic energy (what would be indicated with positive $R(K_{\mathrm{Z}})$). However, it is important to recall that these residual terms include not only frictional dissipation, but also boundary pressure work and contribution from non-resolvable scales. Moreover, there is also a computational uncertainty due to errors accumulated from the calculations of other energy components which are used to obtain residual terms. Although these errors have to be kept in mind, residual terms $R(K_{\mathrm{Z}})$ and $R(K_{\mathrm{E}})$ essentially represent the exchange of kinetic energy between subgrid-scale and grid-scale flows [20]. Therefore, these processes may contribute to the great amount of K_{Z} as it is evident here by the negative value of $R(K_{\mathrm{Z}})$ after 0000 UTC 19 November. It can be concluded that negative $R(K_{\mathrm{Z}})$ also sustain the cyclone since it makes more K_{Z} energy available for conversion to K_{E} through the $C(K_{\mathrm{Z}}, K_{\mathrm{E}})$ process. $R(K_{\mathrm{E}})$ shows an oscillatory character. It acts as a source of K_{E} before the cyclone is formed. When the cyclone and its eddy motion are developed (0000 UTC 19 November), $R(K_{\mathrm{E}})$ is positive indicating that dissipation causes the loss of eddy kinetic energy. This loss is compensated by the other three energy components, $B(K_{\mathrm{E}})$, $C(A_{\mathrm{E}}, K_{\mathrm{E}})$ and $C(K_{\mathrm{Z}}, K_{\mathrm{E}})$ which maintain the cyclone existence. On 1200 UTC 19 November, $R(K_{\mathrm{E}})$ has a negative sign, so it acts as a source of K_{E}. But the other processes (except $C(K_{\mathrm{Z}}, K_{\mathrm{E}})$ which is positive all the time) cause decrease of K_{E}, so the cyclone weakens.

6. – Conclusions

This study presents the energy budget of an area influenced by intense cyclone development during the period 18-21 November 1999. Although the life-cycle of the cyclone was relatively short, its rapid development has an impact on energetics calculated over the limited area. Albeit this study is restricted to the consideration of its contributions to the global budged, the results show that energy contents and their changes in different atmospheric layers are possible to discuss in the course of the cyclone's development.

The results show that the cyclone development has been triggered in the upper atmospheric levels (close to 300 hPa) by strong horizontal and vertical shears of the zonal wind. Conversion $C(K_{\mathrm{Z}}, K_{\mathrm{E}})$ is the most intense on the upper levels, approximately on the 350 hPa isobaric level. It behaved as a strong source of K_{E}, so it has been a crucial process for the development of the studied cyclone. The baroclinity of the middle troposphere has allowed intensive vortex downward propagation, resulting in the surface cyclone on 19 November 1999. The vortex propagation throughout the troposphere is associated with downward K_{E} transport (from the jet stream level toward the surface).

The obtained results could be limited to the ALADIN model, so it is expected that results based on data of some other numerical model would differ to some extent. It is also particularly important to note that results calculated over the sub-domain which encloses only the studied cyclone provided energy contents which are associated with its life cycle. Contrary, the calculation over the whole ALADIN/LACE domain did not result in energetics that reflects cyclone development, perhaps due to the impact of other synoptic disturbances placed over the domain. Therefore, enlargement of the used domain does not necessary improve results, as one may expect.

Although weather conditions in its domain are strongly influenced by Genoa cyclones, it is particularly important to emphasize that ALADIN/LACE model is not generally useful for studying Genoa cyclones. Since the Gulf of Genoa is placed in the lower left corner of ALADIN/LACE domain, some of the cyclones developed there hardly fit into the domain. In such cases, it is not possible to find any sub-domain inside of ALADIN/LACE which encloses the considered system.

Nevertheless, this case study has shown that although the used domain was extremely small, the cyclone development had considerably contributed to the estimated energetics. Furthermore, the analysis of energy contents, as well as conversion and transformation processes, has provided more insights regarding a possible mechanism of its formation.

* * *

The author gratefully acknowledges Dr. N. Šinik for helpful discussions and suggestions. The author is thankful to Dr. Z. Bencetić Klaić for reading the manuscript. ALADIN data were provided by the Meteorological and Hydrological Service of Croatia. This study was supported by the Ministry of Science, Education and Sports of the Republic of Croatia under the Project no. 0119330.

REFERENCES

[1] Lorenz E. N., *Tellus*, **7** (1955) 157.
[2] Muench H. S., *J. Atmos. Sci.*, **22** (1965) 349.
[3] Oort A. H., *Mon. Weather Rev.*, **92** (1964) 483.
[4] Reed R. J., Wolfe J. L. and Nishimoto H. J., *Atmos. Sci.*, **20** (1963) 256.
[5] Desai D. S., *Mausam*, **37** (1986) 365.
[6] George L. and Mishra K., *Q. J. R. Meteorol. Soc.*, **119** (1993) 755.
[7] Rajamani S. and Kulkarni J. R., *Mausam*, **37** (1986) 9.
[8] Singh U. S. and Singh R. K., *Idöjárás*, **96** (1992) 93.
[9] Smith P. J., *Mon. Weather Rev.*, **101** (1973) 757.
[10] Alpert P., Neeman B. U. and Shay-el Y., *Tellus*, **42** (1990) 65.
[11] Herceg I., *Geofizika*, **15** (1998) 15.
[12] Smith P. J., *Tellus*, **21** (1969) 202.
[13] Johnson D. R., *J. Atmos. Sci.*, **27** (1970) 727.
[14] Brennan F. E. and Vincent D. G., *Mon. Weather Rev.*, **108** (1980) 965.
[15] Caian M. and Geleyn J.-F., *Q. J. R. Meteorol. Soc.*, **123** (1997) 743.
[16] Bubnova R., Hello G., Bénard P. and Geleyn J.-F., *Mon. Weather Rev.*, **123** (1995) 515.
[17] Holton J. R., in *An Introduction to Dynamic Meteorology* (Academic Press, London) 2004, pp. 140-180.
[18] Mishra S. K. and Rao V. B., *Q. J. R. Meteorol. Soc.*, **127** (2001) 2329.
[19] Oort A. H. and Peixoto J. P., *J. Geophys. Res.*, **79** (1974) 270.
[20] Ward J. H. and Smith P. J., *Mon. Weather Rev.*, **104** (1976) 836.